Satellite Data Assimilation Using NASA Data Systems Test 6 Observations

YOSHI K. SASAKI AND JAMES S. GOERSS

Cooperative Institute for Mesoscale Meteorological Studies, University of Oklahoma, Norman 73019

(Manuscript received 4 February 1982, in final form 23 July 1982)

ABSTRACT

Two assimilation schemes are described in which continuous indirect insertion of satellite-derived temperatures is performed, using a global primitive equation forecast model. Both schemes employ a relatively simple indirect insertion technique but utilize different methods (Noise Freezing Methods I and II) to control the noise induced within the forecast model by data insertion. Using data collected in February 1976 during NASA Data Systems Test 6, the effectiveness of these schemes is compared with that of a third scheme in which satellite-derived temperatures are assimilated using the same techniques that most operational forecast centers employ. After a 36 h start-up period, 48 h forecasts were produced using each assimilation scheme and root-mean-square errors computed for the differences between the forecast fields and upper-air observations of geopotential height. The forecasts of geopotential height made using the noise freezing methods are found to show substantial improvements over those made using conventional techniques. The forecasts produced using Noise Freezing Methods I and II are comparable with each other, and show average percent improvements over conventional forecasts ranging from 5 to 10% at 850 mb and from 10 to 15% at both 500 and 300 mb. Improvements of nearly 25% are observed for individual forecasts.

1. Introduction

The accuracy of forecasts made by numerical weather prediction models is dependent upon two factors: 1) the ability of the model to realistically represent the atmospheric processes, and 2) the ability to provide the model with initial conditions which reflect the true state of the atmosphere. One of the major goals of data assimilation research has been to solve the second problem. Before the development of satellite-borne measurement systems in the 1960's, the amount of asynoptic data available was limited and data assimilation schemes were designed primarily to handle the conventional surface and upper-air observations. Unlike this conventional data, the vast amount of satellite observations which have become available consist of measurements of meteorological variables (temperature and winds) which are widely distributed in both space and time. Beginning with a paper by Charney *et al.* (1969), a great deal of data assimilation research has been conducted to determine ways to use this new data source. McPherson (1975) and Bengtsson (1975) have provided excellent reviews of this research and have conventionalized the terminology used in the literature. In this paper we will adhere to these conventions.

Dynamic assimilation describes the use of a numerical prediction model as an integrator of observations distributed in time and space. Direct insertion refers to updating the model only at the model grid point nearest the location of the observation, while indirect insertion refers to the process of interpolating the observation to a number of surrounding model grid points using some sort of objective analysis scheme. Further distinction is made between continuous insertion, where the model is updated at the time step nearest the time of observation, and intermittent insertion, where the model is updated at distinct intervals by data stratified into groups.

Early data assimilation experiments were conducted using real data by Hayden (1973) and Gauntlett and Seaman (1974). Both studies involved intermittent indirect insertion into a hemispheric atmospheric model and dealt mainly with the mechanics of data assimilation itself. In each case, indirect insertion was accomplished using the objective analysis techniques introduced by Bergthorsson and Doos (1955) and elaborated upon by Cressman (1959). Two more recent studies using real data collected during the NASA Data Systems Tests have addressed the question of whether satellite data assimilation can have a positive impact upon numerical forecasts. Tracton *et al.* (1980) performed global data assimilation using intermittent indirect insertion and evaluated the results with Northern Hemisphere forecasts. They found the impact of satellite data assimilation to be negligible. On the other hand, a global data assimilation scheme, using continuous indirect insertion, was found by Ghil *et al.* (1979) to have a statistically significant positive impact upon 2–3 day numerical forecasts.

In this study, two global data assimilation schemes

0027-0644/82/111635-10$06.50

using continuous indirect insertion are evaluated. Both schemes employ techniques to control the noise induced by data insertion within a numerical model and are described in detail in the next section. In Section 3, the results of an extensive experiment using data collected during NASA Data Systems Test 6 are presented. Forecasts produced using these two assimilation schemes are compared with those made using a third assimilation scheme, in which intermittent indirect insertion is performed utilizing techniques similar to those employed by most operational forecast centers.

2. Methodology

In this section, the ingredients of a data assimilation scheme suitable for operational use are described. As was pointed out by McPherson (1975), the experiments conducted by Morel *et al.* (1971) indicate that a fully four-dimensional dynamic assimilation scheme is not operationally feasible. The repeated forward and backward integrations required using a sophisticated forecast model would make this method too expensive in terms of computer resources. The scheme we have designed represents a compromise between true four-dimensional assimilation and operational constraints.

Each cycle of our assimilation scheme consists of three stages. First, forward-only assimilation is performed using the asynoptic observations gathered over the 6-h period preceding the current synoptic time (0000, 0600, 1200 or 1800 GMT). Beginning with the initial conditions valid at the previous synoptic time, the forecast model is updated by continuous indirect insertion of the asynoptic data using the objective analysis techniques described by Barnes (1964, 1973). The resulting forecast, valid at the current synoptic time, provides the first-guess fields of meteorological variables to be used in the second stage of the assimilation scheme. The second stage can be termed an intermittent indirect insertion and consists of a three-dimensional variational objective analysis, which combines the new synoptic observations with the first-guess fields to produce an intermediate set of fields. Although some balancing of the mass and momentum fields is provided by the objective analysis, further balancing is achieved by the third stage where dynamic initialization is performed upon these intermediate fields to produce a set of final fields. Thus, the cycle is complete as these final fields are used as the initial conditions for the forecast model at the current synoptic time.

The operations of a conventional forecast center can be simulated by omitting the first stage of the assimilation scheme and simply using the 6-h model forecast fields as the first-guess utilized in the second stage. Then the collection of synoptic observations used by the variational objective analysis would be augmented by the satellite observations in the ±3 h window about the synoptic time. Thus, the only additional computer resources that would be required by a forecast center which utilized continuous dynamic assimilation of asynoptic data, are those needed to make an additional 6-h model forecast. At the same time, a modest reduction in computer resources would be realized by the reduction in the data base utilized by the objective analysis scheme at each synoptic time.

a. Forecast model

The forecast model used in this study is a global, baroclinic primitive equation model with terrain using spherical coordinates (λ, θ) with σ the vertical coordinate. The model is dry, hydrostatic and its equations, written in flux form, are

$$\frac{\partial \pi}{\partial t} + \frac{1}{a\cos\theta}\left[\frac{\partial}{\partial \lambda}(\pi u) + \frac{\partial}{\partial \theta}(\pi v \cos\theta)\right] + \frac{\partial}{\partial \sigma}(\pi \dot{\sigma}) = 0, \quad (1)$$

$$\frac{\partial}{\partial t}(\pi u) + \frac{1}{a\cos\theta}\left[\frac{\partial}{\partial \lambda}(\pi u^2) + \frac{\partial}{\partial \theta}(\pi u v \cos\theta)\right] + \frac{\partial}{\partial \sigma}(\pi u \dot{\sigma}) + \frac{\pi}{a\cos\theta}\left[\frac{\partial \phi}{\partial \lambda} + \sigma\alpha\frac{\partial \pi}{\partial \lambda}\right] - \left[f + \frac{u\tan\theta}{a}\right]\pi v = \pi F_\lambda, \quad (2)$$

$$\frac{\partial}{\partial t}(\pi v) + \frac{1}{a\cos\theta}\left[\frac{\partial}{\partial \lambda}(\pi u v) + \frac{\partial}{\partial \theta}(\pi v^2 \cos\theta)\right] + \frac{\partial}{\partial \sigma}(\pi v \dot{\sigma}) + \frac{\pi}{a}\left[\frac{\partial \phi}{\partial \theta} + \sigma\alpha\frac{\partial \pi}{\partial \theta}\right] + \left[f + \frac{u\tan\theta}{a}\right]\pi u = \pi F_\theta, \quad (3)$$

$$\frac{\partial}{\partial t}(\pi T) + \frac{1}{a\cos\theta}\left[\frac{\partial}{\partial \lambda}(\pi u T) + \frac{\partial}{\partial \theta}(\pi v T \cos\theta)\right] + \left(\frac{p}{1000}\right)^\kappa \frac{\partial}{\partial \sigma}(\pi \dot{\sigma}\theta) + \frac{\pi^2 \sigma \alpha}{c_p} \times \left[\frac{1}{a\cos\theta}\left\{\frac{\partial u}{\partial \lambda} + \frac{\partial}{\partial \theta}(v\cos\theta)\right\} + \frac{\partial \dot{\sigma}}{\partial \sigma}\right] = \frac{\pi Q}{c_p}, \quad (4)$$

where $p = \pi\sigma + p_t$, $\pi = p_s - p_t$, and p_s and p_t represent the values of pressure at the surface and top of the model atmosphere, respectively. The value of p_t is 200 mb. No parameterizations of irreversible physical processes were included in this study.

A staggered grid system, the (C) lattice described in Mesinger and Arakawa (1976), is utilized along with centered-space and centered-time differences. The horizontal resolution is 7.5°, the model time-step

is 450 s, and there are three vertical levels. Mass and total energy are conserved by performing variational adjustments each time-step, as described and demonstrated by Sasaki (1976, 1977) and discussed by Navon (1981). Time-filtering (Robert, 1966; Asselin, 1972) is employed at each time-step to control the high-frequency computational modes induced by the leapfrog time differencing scheme.

In order to ensure computational stability, latitudinal filtering must be performed in the vicinity of the poles, due to the reduction in size of the horizontal grid spacing caused by the equal latitude–longitude grid. In this model, Fourier filtering is applied every time-step to the tendencies of each of the prognostic variables for latitudes poleward from 45°. The maximum wavenumber passed during the filtering is smoothly increased from each pole to 45° latitude.

b. *Variational objective analysis and dynamic initialization*

At each synoptic time, the following three-dimensional variational objective analysis procedure is used to combine the newly acquired upper-air and surface observations with the first-guess fields. Objectively analyzed fields of geopotential height and winds are produced by minimizing the functional

$$J = \int\int\int \Big[A(\phi - \hat{\phi})^2 + B\left(\frac{1}{R}\frac{\partial \phi}{\partial \pi} - \hat{T}\right)^2 + C_u(u - \hat{u})^2 + C_v(v - \hat{v})^2 + d(\nabla\phi - \nabla\tilde{\phi})^2 + e(\nabla^2\phi - \nabla^2\tilde{\phi})^2 + f(\zeta - \tilde{\zeta})^2 + g(D - \tilde{D})^2 + h\left(\frac{1}{a\cos\theta}\frac{\partial\phi}{\partial\lambda} - fv\right)^2 + i\left(\frac{1}{a}\frac{\partial\phi}{\partial\theta} + fu\right)^2\Big] \times d\lambda d\theta d\pi, \quad (5)$$

where

$$\nabla\phi = \frac{1}{a\cos\theta}\frac{\partial\phi}{\partial\lambda} + \frac{1}{a}\frac{\partial\phi}{\partial\theta}$$

$$\nabla^2\phi = \frac{1}{a^2\cos^2\theta}\frac{\partial^2\phi}{\partial\lambda^2} + \frac{1}{a^2\cos\theta}\frac{\partial}{\partial\theta}\left(\cos\theta\frac{\partial\phi}{\partial\theta}\right)$$

$$\zeta = \frac{1}{a\cos\theta}\left(\frac{\partial v}{\partial\lambda} - \frac{\partial(u\cos\theta)}{\partial\theta}\right)$$

$$D = \frac{1}{a\cos}\left(\frac{\partial u}{\partial\lambda} + \frac{\partial(v\cos\theta)}{\partial\theta}\right) \text{ and } \pi = \ln(1000/p).$$

The resulting values of geopotential height, u-wind, and v-wind are denoted by ϕ, u and v, respectively, while their corresponding first-guess field values are denoted by $\tilde{\phi}$, $\tilde{u}$ and $\tilde{v}$. Three-dimensional data weight matrices A, B, C_u and C_v contain relatively high values at locations of observed geopotential height, temperature, u-wind and v-wind ($\hat{\phi}$, $\hat{T}$, $\hat{u}$ and $\hat{v}$) and negligible values elsewhere. The weights d, e, f, g, h and i are constant over most of the domain, but are set to zero near the boundaries in order to satisfy certain boundary conditions. Each weight is assigned a value equal to the inverse of the expected variance of the difference it is associated with in the functional J. These expected variances are estimated by computing the sample variances for each difference, for many different cases. The values of these weights are model-dependent, but should never be permitted to vary from case to case.

The solution of this variational problem over the domain, results in fields of geopotential height, u-wind and v-wind:

1) which agree with the surface and upper-air observations;
2) for which the horizontal gradients and Laplacians of geopotential height and the vorticity and divergence of the wind field match those for the first-guess fields;
3) for which the vertical derivatives of the geopotential height field are consistent with the observed temperatures; and
4) which are in approximate geostrophic balance.

Before the final analysis is produced, the individual weights within data weight matrices A, B, C_u and C_v are evaluated using a procedure based on the work of Holl and Mendenhall (1972). Although this procedure is not as elegant as the cross-validation methods developed by Wahba and Wendelberger (1980), it is computationally more feasible for handling the vast amount of data required for a global analysis. The total objective analysis procedure consists of three passes, each beginning with the minimization of functional (5) by relaxation. Except for gross error checking to eliminate obviously incorrect data from the analysis, the first pass begins with uniformly high weights given to all observations. Subsequent passes will utilize weights whose values have been re-evaluated.

Let us denote dependent variables in general as X and their weight fields (matrices) as W. Before relaxation, $\hat{X}$ fields are constructed from the observations. After relaxation, all new values of the dependent variables are obtained producing an X' field with a resulting unknown weight field W'. For each dependent variable this may be expressed as

$$W'_{ijk}X'_{ijk} = W_{ijk}\hat{X}_{ijk} + \text{ambient information}. \quad (6)$$

That is, the field element $\hat{X}_{ijk}$ with weight W_{ijk} is altered during relaxation by adding some unknown ambient information. In order to re-evaluate the weights we must determine the weight field W'. If we assume that a small change in $\hat{X}_{ijk}$ will produce a change in X'_{ijk} without altering the ambient information, we have

$$W'_{ijk}(X'_{ijk} + \delta X'_{ijk}) = W_{ijk}(\hat{X}_{ijk} + \delta\hat{X}) + \text{ambient information}. \quad (7)$$

Subtracting (6) from (7), we obtain

$$\left.\begin{aligned} W'_{ijk}\delta X'_{ijk} &= W_{ijk}\delta\hat{X} \\ W'_{ijk} &= W_{ijk}\cdot\delta\hat{X}/\delta X'_{ijk} \end{aligned}\right\}, \quad (8)$$

where the only unknown in (8) is $\delta X'_{ijk}$. To determine $\delta X'_{ijk}$, a perturbation $\delta\hat{X}$ is added to the $\hat{X}$ field at grid point (i, j, k) and the relaxation procedure is repeated. Since this must be done for each grid point which is influenced by an observation, it is impractical to perform the relaxation over the entire domain. Instead, it is performed over only the 3×3 grid centered on grid point (i, j, k), except when that grid point is located along the boundary of the domain and the 3×3 grid inboard from the boundary is used. The values obtained from the last relaxation over the entire domain are used as boundary conditions. We denote the result of this nine-point relaxation by X^*_{ijk} and obtain $\delta X'_{ijk}$ by merely subtracting X'_{ijk} from X^*_{ijk}. Thus, the value of W'_{ijk} can now be directly computed from (8).

Once the W' field has been obtained, the data weight re-evaluation can proceed. The quality of each observation is judged by the degree to which the analysis is dependent upon it. If the analysis is much different when a particular report is withheld, that report will be considered unreliable. To determine the impact of a report, consider Eq. (6). In reality, the ambient information affecting grid point (i, j, k) is influenced by the value $\hat{X}_{ijk}$, but, in an approximate sense, we can ignore this dependency and view the relaxation process as a linear combination of $W_{ijk}\hat{X}_{ijk}$ and some other unspecified terms. Now $\hat{X}_{ijk}$ is itself a linear combination of the first-guess field and all observations which influenced the (i, j, k)th grid point. Within this approximation, the analyzed value with report X_n withheld is

$$X^B_{ijk} = (W'_{ijk}X'_{ijk} - W_nX_n)/W^B_{ijk},$$

where W_n is the weight currently assigned to report X_n and W^B_{ijk} is given by

$$W^B_{ijk} = W'_{ijk} - W_n.$$

We refer to X^B_{ijk} as the background analysis value of report X_n and W^B_{ijk} as the background weight.

Recalling that the weights represent the inverse of variance, in the expected sense the standard deviation of the difference between a report X_n and its background value X^B_{ijk} is

$$E = (1/W^B_{ijk} + 1/W_n^0)^{1/2},$$

where W_n^0 is the class weight for reports of the type to which report X_n belongs. The fact that the weight for a particular report may have been reduced does not alter this expected quantity. If the actual difference between X_n and its background value exceeds the expected standard deviation, then the weight W_n will be reduced from W_n^0 for the next pass. This is accomplished by examining the value of

$$\lambda^2 \equiv (X_n - X^B_{ijk})^2/E^2.$$

If $\lambda^2 \leq 1$, then report X_n will be given its full weight W_n^0 on the next pass. If $\lambda^2 > 1$, then the weight W_n will be reduced by the formula

$$W_n = 2W_n^0/(1 + \lambda^2).$$

At the beginning of each pass, the weight for each report has a chance to return to its original weight W_n^0, and the weight given to the report for the next pass is independent of the weight it had on the previous pass.

Thus, after each of the first two passes of the objective analysis procedure, all data weights are re-evaluated. At the end of the first pass some of these weights may be reduced from the uniformly high values they were assigned at the beginning of that pass. The second pass is performed so that some of these weights may be partially or totally restored if the observations they are associated with are supported by other data. The final analysis is then produced by minimizing (5) using these weights. Typically, ~75% of the observations will retain their original weights, ~20% will experience minor weight adjustment, and the remaining fraction will undergo substantial weight reduction.

The dynamic initialization used to complete each cycle of the assimilation scheme is a relatively simple one which we refer to as "internal balancing". One can combine (2) and (3) to produce a prognostic equation for mass divergence. Beginning with the intermediate fields, which result from the objective analysis procedure, the forecast model is run forward several time steps. Using the resulting mass divergence tendencies, adjustments are made to the temperature (geopotential height) field so that the initial divergence tendency is zero. In order to show the effectiveness of the initialization, 12-h forecasts were made from the same set of initial conditions with and without internal balancing. The two solid lines in Fig. 1 show the results of computing the global root-mean-square (rms) pressure tendency at each forecast time step. It can be seen that the dynamic initialization procedure results in approximately a factor of two reduction of this quantity, indicating a significant reduction in the gravitational noise which is induced by unbalanced initial fields. The geopotential height fields which result from internal balancing are only subtly different from their unbalanced counterparts and typically display root-mean-square error (rmse) increases of less than 2 m at 850 mb and of ~5 m at 500 mb when compared with the upper-air observations.

c. Dynamic assimilation techniques

The major problem encountered in employing dynamic assimilation techniques is retaining the information contained in the asynoptic observations in face of the model "shock" caused by their insertion. An excellent description of this shock is given by Miyakoda *et al.* (1978). When asynoptic data are inserted into an atmospheric model, they create discontinuity with the current model solution. The dynamical characteristics of the fluid enable it to remove this discontinuity in such a way as to maintain a state of approximate geostrophic balance. This geostrophic adjustment process results in the generation and dispersal of inertia gravity waves. As was pointed out by Talagrand (1972), the effectiveness of an assimilation scheme is dependent not only on the amount of information introduced into the model, but also upon how well the high-frequency noise caused by this introduction can be damped.

An extreme example of this problem was illustrated by Talagrand and Miyakoda (1971) who found that direct insertion of simulated data into a balanced barotropic model resulted in numerical instability. The conclusion of two other studies using simulated asynoptic data is that indirect insertion accelerates the assimilation process (Bengtsson and Gustavsson, 1971; Miyakoda and Talagrand, 1971). The spreading of information contained in an observation to several surrounding model grid points, using some sort of objective analysis technique, was found to increase the effectiveness of assimilation. In fact, in an extensive assimilation experiment using real data and a number of indirect insertion schemes, Ghil *et al.* (1979) found that the success of assimilation (based on forecast improvement) was directly related to the level of sophistication of the insertion scheme used. The implication is that the more sophisticated insertion schemes are capable of introducing more information into the model, with less resulting shock. The consensus of a number of other assimilation studies using both real and simulated asynoptic data is that the assimilation process is also accelerated by some sort of static balancing (Rutherford and Asselin, 1972; Hayden, 1973; Halberstam, 1974; Kistler and McPherson, 1975; Miyakoda *et al.*, 1978). By static balancing, we refer to the local balancing of mass and motion fields in the area of data insertion.

In all of the previously mentioned papers, the insertion problem has been attacked by minimizing or

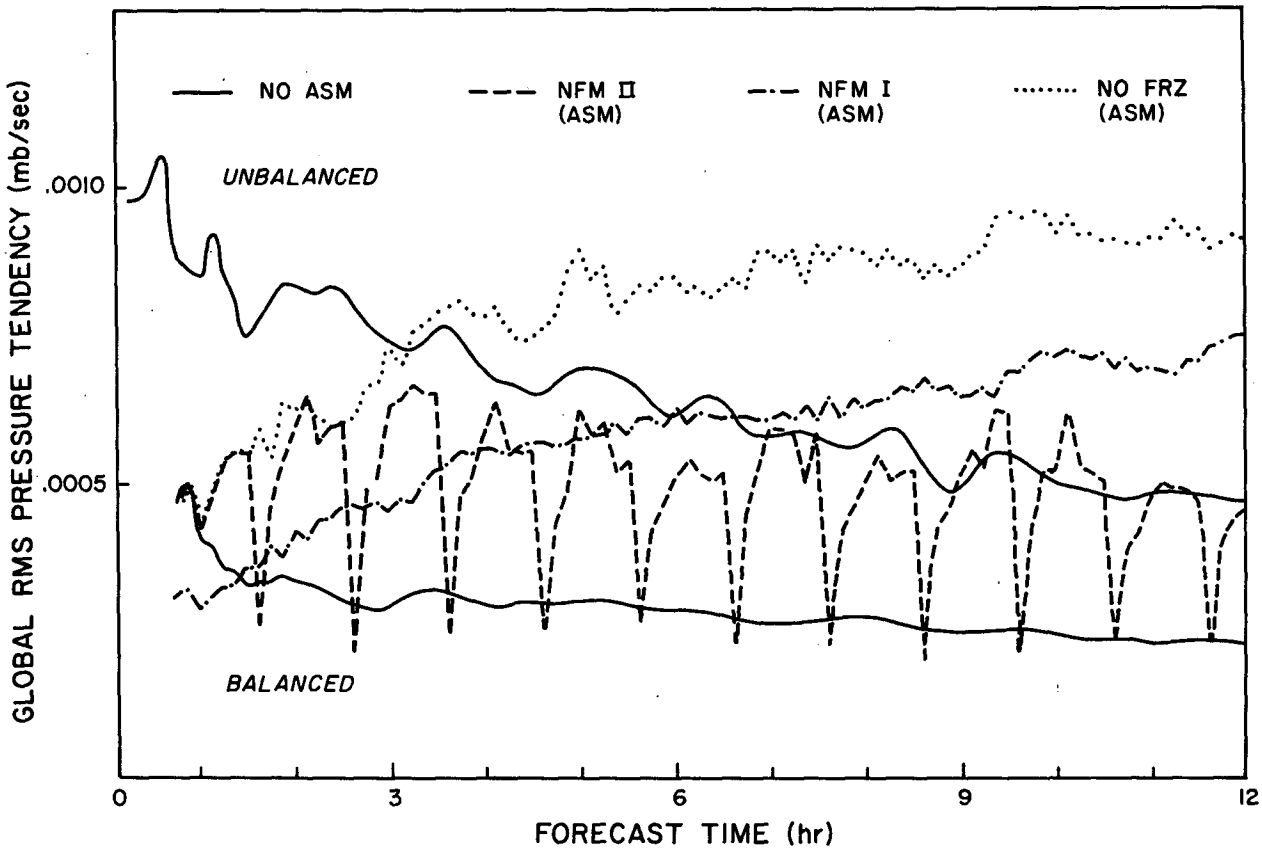

FIG. 1. Globally averaged root-mean-square pressure tendencies for balanced and unbalanced non-assimilation forecasts and balanced assimilation forecasts.

reducing the shock at the time of insertion. We have approached the problem from a different viewpoint. In this study, we have used a simple indirect insertion scheme (Barnes, 1964, 1973) but controlled the noise produced after insertion. Two different noise control techniques, which we term Noise Freezing Methods I and II, are examined.

During the first stage of our assimilation scheme, the forecast model is updated by continuous indirect insertion of asynoptic data. This insertion is accomplished each time step in the following fashion. Let K represent the number of asynoptic observations taken during a block of time, within radius R of a model grid point. In this study R was chosen to be 1000 km. This block of time is centered about the end of the model time step, and has the same length as the model time step. For each time step, a two-pass Barnes analysis is performed. On the first pass, the forecast temperature T_f, at each grid point, is replaced by

$$T = T_f + [\sum_{i=1}^{K} W_i(T_i - T_{fi})/\sum_{i=1}^{K} W_i],$$

where T_i is the observed temperature at the pressure level of the grid point and T_{fi} is the forecast temperature interpolated to the location and pressure level of the observation. The weight associated with the observation is

$$W_i = \exp[-D_i^2/(\gamma\beta^2)],$$

where D_i is the distance from the grid point to the location of the ith observation. Using the curves produced by Buell (1972), β is chosen to be 800 km to limit the influence of an observation to an area which approximately corresponds to positive values of the correlation structure functions. The process is repeated on the second pass with the value of γ reduced from 1.0 to 0.3 and with the forecast values being replaced with the results of the first pass.

In a barotropic model, the speed of the gravitational modes is proportional to the square root of the mean atmospheric depth. By reducing the modeled mean depth, the gravitational modes are slowed without substantially affecting the waves of meteorological significance. This phase speed reduction results because the contribution of horizontal divergence to changes in the depth of the fluid is decreased. We refer to this phenomenon as "noise freezing." The implementation of noise freezing in a baroclinic model requires the contribution of horizontal divergence to the surface pressure tendency to be reduced without disrupting the horizontal gradients of π. This is most easily done by subtracting a constant from all values of π carried within the forecast model. The noise freezing constant is chosen to be as large as possible without causing negative or zero values of π. In this study, the value was selected to be 400 mb. Since the equations of motion and the thermodynamic equation used in the model are written in flux form by adding the continuity equation, care must be taken so that the reduction of π does not improperly affect the values of other variables in the equations. The noise freezing constant must be added to π whenever π is used, to diagnose the values of ϕ and α in (2) and (3) and the values of P, θ and α in (4). When these exceptions have been accounted for, the model can be run with noise freezing by simply subtracting the constant from the initial values of π. We refer to the technique of performing dynamic assimilation with the forecast model modified in this fashion as Noise Freezing Method I (NFM-I).

In order to demonstrate the effect of NFM-I, the model was subjected to a large shock by reducing the temperatures at all three levels by 20°C at 33.75°N, 90°E. Beginning with the same set of initial conditions, frozen and unfrozen forecasts were run with and without this shock. Fig. 2 displays the difference field (shocked minus unshocked) for 1-h unfrozen forecasts of π. The central value of the high exceeds

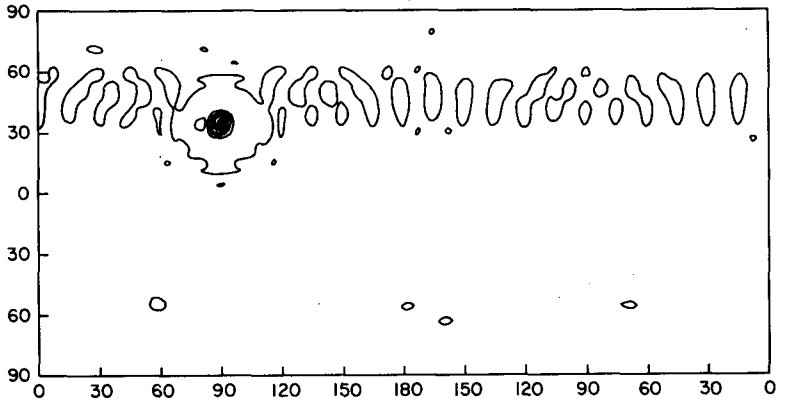

FIG. 2. Difference field (mb) between 1-h unfrozen surface pressure forecasts (shocked minus unshocked).

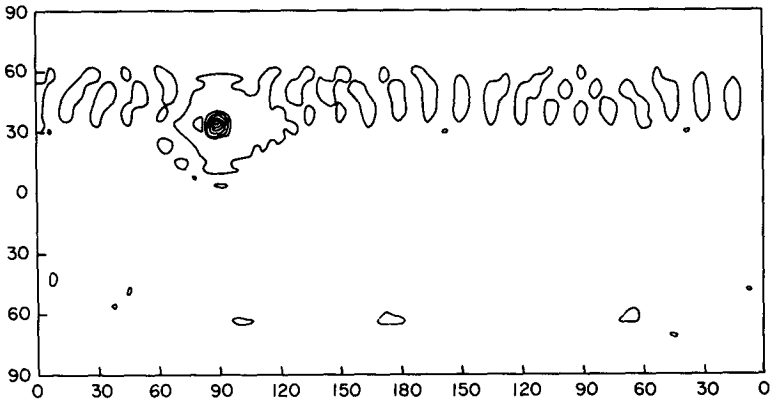

FIG. 3. As in Fig. 2, but for 3-h frozen surface pressure forecasts.

48 mb. The difference field for 3-h *frozen* forecasts of π is shown in Fig. 3, where the central value of the high is just above 40 mb. It can be seen that noise freezing has reduced the phase speed of the gravity waves by almost a factor of three. In both figures, a suspicious belt extends around the globe, centered approximately at 45°N. This is the direct result of the Fourier filtering performed in the model poleward from 45°N. A similar plot for the 3-h unfrozen forecasts is displayed in Fig. 4. It can be seen that the central value of the high has diminished to ~24 mb, and that the radius of influence of the noise is approximately three times as large as that in Figs. 2 and 3.

The effect of NFM-I upon the insertion of asynoptic data into the forecast model is two-fold. First, by slowing the gravitational modes induced by the insertion shock, it limits the propagation of this noise throughout the model. Second, by localizing the geostrophic adjustment process with these modes, more asynoptic information is incorporated into the model.

The second noise control technique considered in this paper is referred to as Noise Freezing Method II (NFM-II). If we define a mass velocity potential such that

$$\pi u = \frac{1}{a\cos\theta}\frac{\partial \chi}{\partial \lambda}, \tag{9a}$$

and

$$\pi v = \frac{1}{a}\frac{\partial \chi}{\partial \theta}, \tag{9b}$$

then

$$\nabla^2 \chi = \left(\frac{1}{a\cos\theta}\right)\left[\frac{\partial}{\partial \lambda}(\pi u) + \frac{\partial}{\partial \theta}(\pi v \cos\theta)\right] = D. \tag{10}$$

At each model level, the mass divergence field D can be high-pass filtered in space to produce a filtered field D'. Using D' as the forcing function, (10) can easily be solved and wind adjustments computed using (9a) and (9b). These wind adjustments are then subtracted from the model wind fields. Periodically during the dynamic assimilation process, this procedure, which is equivalent to low-pass filtering the mass divergence fields and adjusting the model wind fields to agree with the smoothed mass divergences, is performed. Thus, the amplitudes of the high frequency waves associated with the gravitational noise are reduced while those for the longer waves are left

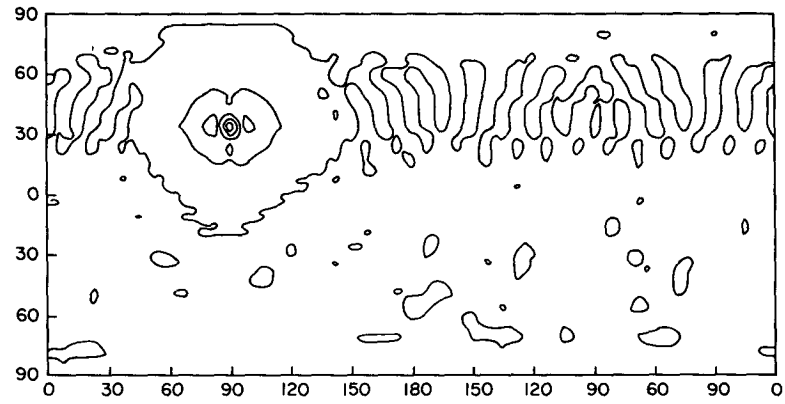

FIG. 4. As in Fig. 2, but for 3-hour unfrozen surface pressure forecasts.

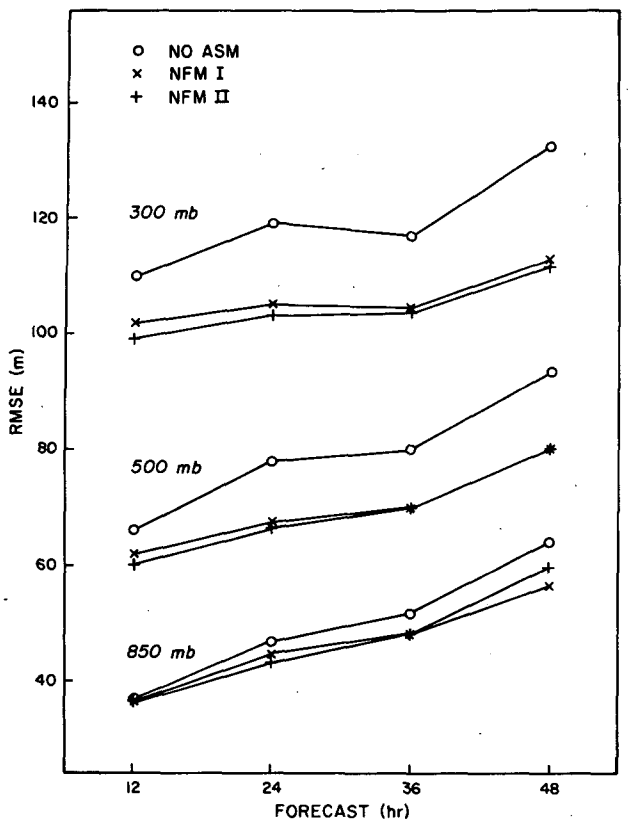

FIG. 5. Average root-mean-square errors (m) for global forecasts made at 1200 GMT 2, 5 and 8 February 1976.

unchanged. The wind adjustment then accelerates the balancing of the model fields.

Beginning with the balanced set of initial conditions used to demonstrate the dynamic initialization procedure discussed in Section (2b), 12-h assimilation forecasts using these methods were made using NFM-I, NFM-II, and without any noise freezing technique. The global rms pressure tendencies for these forecasts are plotted in Fig. 1. After three hours, the steadily increasing noise level of the forecast made without noise freezing has reached that of the forecast made from unbalanced initial conditions. The noise level for the forecast made using NFM-I is also steadily increasing, but takes six hours to reach the level of the unbalanced forecast. Despite its saw-tooth pattern, the overall noise level tends to remain relatively steady over the forecast period when NFM-II is implemented.

3. Experimental results

Using data collected in February 1976 during NASA Data Systems Test 6, the effectiveness of three different assimilation schemes was tested. The asynoptic observations used in these tests were the operational Vertical Temperature Profile Radiometer (VTPR) soundings of NOAA-4, and the experimental retrievals obtained from the combination of the High Resolution Infrared Sounder (HIRS) and Scanning Microwave Spectrometer (SCAM) radiance data of Nimbus-6. As described in the previous section, two of the schemes involved continuous assimilation of the asynoptic observations, using indirect insertion and the application of either NFM-I or NFM-II. The third scheme (NO ASM) was patterned after the operations of a conventional forecast center. The only differences among these schemes were the contents of the first-guess fields and the data base used in the objective analyses performed each synoptic time. For NO ASM, these first-guess fields were merely the 6-h model forecast valid at the synoptic time while the data base included the satellite observations in the ±3 h window about that time. The results of the respective dynamic assimilations served as the first-guess fields for NFM-I and NFM-II, and no asynoptic observations were included in the objective analysis data base.

After a 36-h start-up period, beginning with three sets of initial conditions (0000 GMT on 1, 4 and 7 February), 48-h forecasts were produced for each assimilation scheme at 1200 GMT on 2, 5 and 8 February. These forecasts were evaluated by computing rmse's of the differences between actual upper-air observations of geopotential height and the values of the forecast fields interpolated to the location and level of these observations. The averages of these rmse's computed over the entire globe for the three assimilation schemes are plotted in Fig. 5. For each forecast period and each vertical level, the forecasts produced using dynamic assimilation of the satellite temperatures, possessed smaller average rmse's than those produced using the conventional approach. In general, the rmse reduction increased with height and forecast length.

Next, a percent improvement for each assimilation forecast (NFM-I or NFM-II) was determined by subtracting its rmse from the NO ASM rmse and then dividing this difference by the NO ASM rmse. The results of these tabulations for geopotential height forecasts are shown in Fig. 6, where the means and range of improvement are plotted. In terms of percent improvement, we can see that both the NFM-I and NFM-II forecasts show a definite improving trend with respect to forecast length. On the average, the improvement for the noise freezing forecasts was ~5% at 850 mb and between 10–15% at both 500 and 300 mb. Over the 48-h forecast period, the improvement for the noise freezing forecasts ranged from slightly more than 0% to almost 10% at 850 mb, and from slightly more than 5% to almost 15% at both 500 and 300 mb. Individual forecast improvements between 20 and 25% were recorded by both noise freezing techniques, with only a few forecast degradations which occurred with 12-h NFM-I forecasts and 12- and 24-h 850 mb forecasts made using

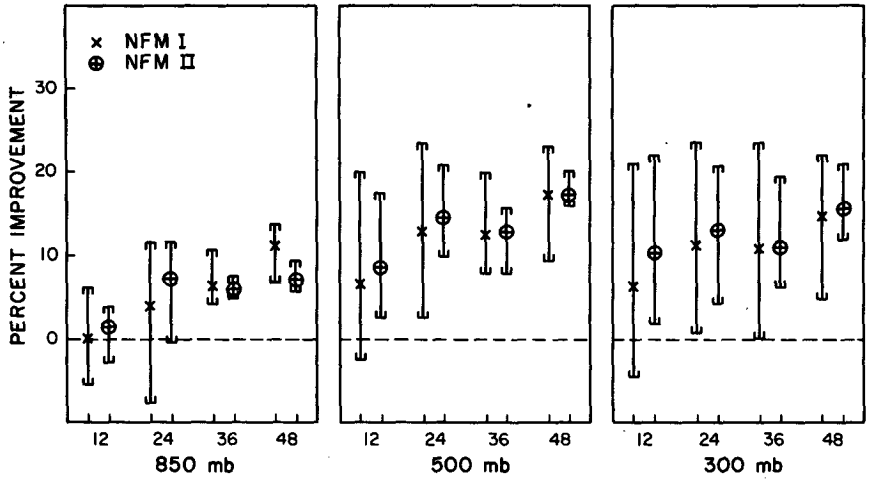

FIG. 6. Average and range of percent improvement over conventional forecasts for global forecasts made using continuous satellite data assimilation at 1200 GMT 2, 5 and 8 February 1976.

both techniques. The range of forecast improvements was consistently smaller for the NFM-II forecasts, while the largest individual forecast improvements were produced using NFM-I. From these results, we can conclude that overall, the forecasts produced using NFM-I and NFM-II are comparable, with those produced using NFM-II being slightly more consistent.

To determine whether the forecast improvements indicated by Figs. 5 and 6 are statistically significant, we examined the differences obtained by subtracting the rmse for an assimilation forecast from that for the corresponding NO ASM forecast. For each length forecast and each level, we can compute three differences. Based on the correlation functions determined by Gandin (1963) and assuming a typical speed of movement of 10 m s^{-1} for weather systems, one can estimate that the sampling time for independent atmospheric states is ~3–5 days. These forecasts were made three days apart so that we could assume independence. To test the hypothesis that the population mean of these differences is zero (no forecast improvement) versus the alternative hypothesis that the population mean is greater than zero (forecast improvement), we use the test statistic

$$t = \bar{x}(n-1)^{1/2}/s, \qquad (11)$$

where $\bar{x}$ is the sample mean of the differences, s is the sample standard deviation, and n is the sample size (Hoel, 1962). This test statistic possesses a Student's t distribution with $n-1$ degrees of freedom. Using this test, we found that all 36- and 48-h forecasts and the 24-h NFM-II forecasts at 500 and 300 mb showed improvement significant at the 95% level. The forecast improvement for all but the 12-h NFM-I forecasts, the 12-h NFM-II forecast at 850 mb, and the 24-h NFM-I forecast at 850 mb were found to be significant at the 90% level.

4. Conclusions

Based on the forecast comparisons described in Section 3, we conclude that substantial forecast improvements can result from global satellite data assimilation using continuous indirect insertion. These results, coupled with those of Ghil *et al.* (1979) and Tracton *et al.* (1980), suggest that the use of continuous, rather than intermittent, data insertion may be the key to successful satellite data assimilation. Both noise control techniques investigated in this study proved to be effective with NFM-II being the more consistent of the two. However, we must temper these positive results with the fact that the variational objective analysis scheme we have used is rather unique. Comparisons with other more widely used objective analysis schemes are underway, to ensure that the results presented here are not due to the use of this scheme.

In this study, we used a relatively simple indirect insertion scheme and did not employ static balancing. Ghil *et al.* (1979) found a direct relationship between forecast improvement and the sophistication of the indirect insertion scheme used, while, as mentioned previously, many researchers found that static balancing accelerated the assimilation process. Further investigation is ongoing to determine whether even more forecast improvement can result by combining these elements with NFM-I or NFM-II.

Finally, it was shown by Charney *et al.* (1969) in a study using simulated data, that the wind field could be induced from the temperature field, even in the tropics, if the error of observation were sufficiently small. However, the error size required was much less

than could be realistically expected from satellite soundings and it was suggested that temperature gradient information might be utilized instead. We have developed a variational indirect insertion scheme which employs satellite temperature gradients rather than absolute temperature values. We are currently testing this scheme to see whether it can produce forecast improvement, especially in the tropical regions.

Acknowledgments. This research was supported by the National Science Foundation and the National Oceanic and Atmospheric Administration through Grant ATM-7824892, and by the Office of Naval Research through Contract N00014-79-C-0758.

REFERENCES

Asselin, R., 1972: Frequency filter for time integrations. *Mon. Wea. Rev.*, **100,** 487–490.

Barnes, S., 1964: A technique for maximizing details in numerical weather map analysis. *J. Appl. Meteor.*, **3,** 396–409.

——, 1973: Mesoscale objective map analysis using weighted time-series observations. NOAA Tech. Memo. ERL NSSL-62, 60 pp. [NTIS COM-73-10781].

Bengtsson, L., 1975: 4-dimensional assimilation of meteorological observations. GARP Publ. Ser., No. 15, 76 pp.

——, and N. Gustavsson, 1971: An experiment in dynamic analysis. *Tellus*, **23,** 328–336.

Bergthorsson, P., and B. Doos, 1955: Numerical weather-map analysis. *Tellus*, **7,** 329–340.

Buell, C., 1972: Correlation functions for wind and geopotential on isobaric surfaces. *J. Appl. Meteor.*, **11,** 51–59.

Charney, J., M. Halem and R. Jastrow, 1969: Use of incomplete historical data to infer the present state of the atmosphere. *J. Atmos. Sci.*, **26,** 1160–1163.

Cressman, G., 1959: An operational objective analysis system. *Mon. Wea. Rev.*, **87,** 367–374.

Gandin, L. S., 1963: Objective analysis of meteorological fields. Transl. from Russian by Israel Prog. for Sci. Transl., 1965, 242 pp. [NTIS TT-65-50007].

Gauntlett, D., and R. Seaman, 1974: Four-dimensional data assimilation experiments in the Southern Hemisphere. *J. Appl. Meteor.*, **13,** 845–853.

Ghil, M., M. Halem and R. Atlas, 1979: Time-continuous assimilation of remote-sounding data and its effect on weather forecasting. *Mon. Wea. Rev.*, **107,** 140–171.

Halberstam, I., 1974: A study of three finite difference schemes and their role in asynoptic meteorological data assimilation. *J. Atmos. Sci.*, **31,** 1964–1973.

Hayden, C., 1973: Experiments in the four-dimensional assimilation of Nimbus 4 SIRS data. *J. Appl. Meteor.*, **12,** 425–435.

Hoel, P., 1962: *Introduction to Mathematical Statistics.* Wiley, 427 pp.

Holl, M., and B. Mendenhall, 1972: Fields by information blending. Tech. Note No. 72-2, Fleet Numerical Weather Central, Monterey, 66 pp. [NTIS AD-A094 082].

Kistler, R., and R. McPherson, 1975: On the use of a local wind corrections technique in four-dimensional data assimilation. *Mon. Wea. Rev.*, **103,** 445–449.

McPherson, R., 1975: Progress, problems, and prospects in meteorological data assimilation. *Bull. Amer. Meteor. Soc.*, **56,** 1154–1166.

Mesinger, F., and A. Arakawa, 1976: Numerical methods used in atmospheric models. GARP Publ. Ser. No. 17, Vol. 1, 66 pp.

Miyakoda, K., and O. Talagrand, 1971: The assimilation of past data in dynamical analysis: I. *Tellus*, **23,** 310–317.

——, R. Strickler and J. Chludzinski, 1978: Initialization with the data assimilation method. *Tellus*, **30,** 32–54.

Morel, P., G. Lefevre and G. Rabreau, 1971: On initialization and non-synoptic data assimilation. *Tellus*, **23,** 197–206.

Navon, I., 1981: Implementation of *a posteriori* methods for enforcing conservation of potential enstrophy and mass in discretized shallow-water equations models. *Mon. Wea. Rev.*, **109,** 946–958.

Robert, A., 1966: The integration of a low-order spectral form of the primitive equations. *J. Meteor. Soc. Japan*, **44,** 237–245.

Rutherford, I., and R. Asselin, 1972: Adjustment of the wind field to geopotential data in a primitive equation model. *J. Atmos. Sci.*, **29,** 1059–1063.

Sasaki, Y., 1976: Variational design of finite-difference schemes for initial value problems with an integral invariant. *J. Comput. Phys.*, **21,** 270–278.

——, 1977: Variational design of finite-difference schemes for initial value problems with a global divergent barotropic model. *Beitr. Phys. Atmos.*, **50,** 284–289.

Talagrand, O., 1972: On the damping of high-frequency motions in four-dimensional assimilation of meteorological data. *J. Atmos. Sci.*, **29,** 1571–1574.

——, and K. Miyakoda, 1971: The assimilation of past data in dynamical analysis, II. *Tellus*, **23,** 318–327.

Tracton, M., A. Desmarais, R. Van Haaren and R. McPherson, 1980: The impact of satellite soundings on the National Meteorological Center's analysis and forecast system—the Data Systems Test results. *Mon. Wea. Rev.*, **108,** 543–586.

Wahba, G., and J. Wendelberger, 1980: Some new mathematical methods for variational objective analysis using splines and cross validation. *Mon. Wea. Rev.*, **108,** 1122–1143.

END OF SPECIAL SECTION